IEEE Access
Multidisciplinary | Rapid Review | Open Access Journal

Received October 8, 2019, accepted October 29, 2019, date of publication November 5, 2019, date of current version November 15, 2019.

Digital Object Identifier 10.1109/ACCESS.2019.2951608

Stochastic Geometry Analysis of Individual Carrier Sense Threshold Adaptation in IEEE 802.11ax WLANs

MOTOKI IWATA[1], (Student Member, IEEE), KOJI YAMAMOTO[1], (Member, IEEE), BO YIN[1], (Student Member, IEEE), TAKAYUKI NISHIO[1], (Member, IEEE), MASAHIRO MORIKURA[1], (Member, IEEE), AND HIRANTHA ABEYSEKERA[2], (Member, IEEE)

[1]Graduate School of Informatics, Kyoto University, Kyoto 606-8501, Japan
[2]NTT Access Network Service Systems Laboratories, NTT Corporation, Yokosuka 239-0847, Japan

Corresponding author: Koji Yamamoto (kyamamot@i.kyoto-u.ac.jp)

ABSTRACT This paper discusses the impact of spatial reuse and carrier sense threshold (CST) optimization on the performance of wireless local area networks using stochastic geometry analysis. The adjustment of the CST is a promising approach to improve spatial reuse, and has been proposed for the IEEE 802.11ax standard. Considering the situation where each access point (AP) individually adjusts its CST based on the individual received power, this paper derives the probability of transmission success and the density of successful transmissions (DST). The evaluation results of these metrics reveal that the optimal setting is to increase the CST linearly (in terms of dB) with respect to the average received signal power. Because the maximization of the DST causes unfairness from the viewpoint of success of transmission, the maximization of the product of the transmission success probabilities is proposed to improve the performance of the entire system and restrain unfairness. Using the trend of the optimal CST function, the impact of the density of APs on the optimal CST function is determined. Moreover, individual CST adjustment is found to improve spatial reuse compared with identical adjustment, i.e., setting the CST of all APs to an identical value.

INDEX TERMS Spatial reuse, carrier sense threshold, inversely proportional setting, IEEE 802.11ax, stochastic geometry.

I. INTRODUCTION

Traffic on wireless local area networks (WLANs) has considerably increased in recent years, and ever more access points (APs) are thus being deployed. However, this does not necessarily increase the aggregated throughput because of the use of the carrier sense multiple access/collision avoidance (CSMA/CA) algorithm. In this algorithm, only one of the APs that share a given channel can transmit at a time.

Adjustment of the carrier sense threshold (CST) is a promising approach to enhance spatial reuse and improve the throughput performance. This is because increasing the CST reduces the number of APs competing with one another and provides high transmission opportunity for each AP. On the contrary, an unnecessarily large CST causes packet collisions owing to harmful interference and, hence, optimizing the CST value is challenging. As a setting of the CST, dynamic sensitivity control, in which APs or stations (STAs) adjust their CST based on the average received power from their associated AP or STA, has been suggested [1], [2]. In dynamic sensitivity control, the CST is set to increase with the received power from the communicating AP or STA. Setting the CST according to the dynamic sensitivity control is said to achieve high spatial reuse and improve the throughput performance [1], [3]. However, adapting the CST alone in dynamic sensitivity control causes an asymmetric carrier sensing relationship and results in throughput starvation [4]. The detail is discussed below.

The inversely proportional setting (IPS) is a promising approach for restraining an asymmetric carrier sensing relationship caused by adjusting the CST alone [4], [5]. The asymmetric carrier sensing relationship causes throughput

The associate editor coordinating the review of this manuscript and approving it for publication was Nan Wu.

starvation because, for example, some APs always detect the medium as busy because other APs that set high CSTs continue to transmit. To solve this problem, the IPS, which restrains the asymmetric carrier sensing relationship, was proposed [4], [5]. In the IPS, all APs keep the product of CST and transmission power constant. Actually, the previous studies [6], [7] experimentally confirmed that the IPS improves the sum throughput where two communication pairs exist.

The performance of the dynamic sensitivity control and IPS is improved further by optimizing the CST, and many studies have been conducted on CST optimization, some even based on stochastic geometry [8]–[10]. In [8], the optimal CST was numerically obtained, and in [9], a method to set the CST based on the density of transmitters in WLANs was proposed in cognitive wireless networks where secondary users are transmitters in WLANs. The method proposed in [10] optimizes the CST by deriving the throughput analytically, assuming that one AP or all APs whose locations follow a Poisson point process (PPP) adopt the identical CST value. As mentioned above, the performance in terms of dynamic sensitivity control has been analyzed. However, to the best of our knowledge, no research to date has studied it adopting the IPS when each AP adjusts its transmission power at the same time as the CST. Although the previous study [10] analyzed the IPS performance, APs are not assumed there to set non-identical CSTs based on each received power. Note that individual CST adjustment improves the network performance compared to identical adjustment because of its higher degree of freedom.

Considering the above-mentioned reason, this paper assumes that the CST and transmission power are set according to the IPS, and analyzes the system performance of IPS where each AP *individually* adjusts its CST and transmission power based on the power it receives. In detail, this paper derives the transmission success probability and density of successful transmissions (DST) based on stochastic geometry analysis presented in [11], and validates the derivations through numerical results. The DST is a system performance metric represented by the product of the density of APs, medium access probability (MAP), and coverage probability (CP), and expresses the mean number of APs whose transmission is successful based on signal-to-interference-plus-noise power ratio.

This paper also determines the optimal CST based on the derived transmission success probability and DST. To improve spatial reuse, it is necessary for each AP's transmission to succeed as evenly as possible while increasing the DST by setting the CST. The issue is formulated as optimization problems and the optimal CST is obtained by solving them. By adopting a step function, the trend of the optimal CST as a function of the average received power is determined.

The contributions of this paper are as follows:

- Compared to stochastic geometry analysis of the MAP, CP, and DST presented in [11], this paper enables analysis assuming *individual* CST adjustment according to the average received signal power.
- This paper shows the optimal CST as a function of average received signal power that maximizes the product of transmission success probabilities to enhance fairness among STAs. It is revealed that the optimal CST is increased *linearly* (in terms of dB) with respect to the received signal power.

TABLE 1. Notation.

Φ	Locations of APs following PPP
λ	Density of APs
x_k	Coordinate of AP k
y_k	Coordinate of STA associated with AP k
r	Communication distance
$f_x(x)$	Probability density function (pdf) of random variable x
$F_x(x)$	Distribution function of random variable x
p_k	Transmission power of AP k
A	Propagation loss at distance of 1 m
α	Path loss exponent
$\|\cdot\|$	Euclidean distance
$h^z_{x_k}$	Fading coefficient between AP or STA at z and AP k
r_k	Communication distance between AP k and associated STA
P	Initial transmission power of all APs
Θ	Initial CST of all APs
$p(\cdot)$	Transmission power function of communication distance
$\theta(\cdot)$	CST function of communication distance
m, m_k	Random backoff time
e_k	Medium access indicator
$\tilde{\Phi}$	$:=\{(x,r,m)\}$ Marked PPP of APs attempting to transmit
$\tilde{\Phi}'$	Marked point process of transmitting APs
$\tilde{\Phi}''$	Marked point process of transmitting APs approximated to PPP
$\mathbb{1}(\cdot)$	Indicator function
T	SINR threshold for correct signal reception
$SINR_k$	SINR at STA associated with AP k
I_k	Sum of interference at STA associated with AP k
σ^2	Noise power
$n(\cdot)$	Defined in (11)
$\mathcal{L}_{I_0}(\cdot)$	Laplace transform of I_0
a	Maximum increment in CST
c	Parameters of $\theta^{(1)}(r)$ in (18)
b_i, l_i	Parameters of $\theta^{(3)}(r)$ in (20)
d_i	Transmission success probability of APs whose communication distance is between l_i and l_{i+1} to all APs
s_i	Ratio of APs whose communication distance is between l_i and l_{i+1} to all APs
c_1, c_2	Parameters of $\theta^{(4)}(r)$ in (26)
$d(r)$	Transmission success probability of AP with communication distance r
$\Lambda(\cdot)$	Intensity function

The rest of this paper is organized as follows. Section II describes the system model, and Section III derives the MAP, CP, and DST, and presents the numerical results. The trend of the optimal CST for the received power is obtained in Section IV. Section V determines the optimal CST for the density of APs. The conclusions of this paper are provided in Section VI.

II. SYSTEM MODEL

The notation used here is summarized in Table 1. Downlink transmission from AP to STA as shown in Fig. 1 is assumed in this paper. This paper focuses on the set of APs that share a given channel and attempt to transmit at a given time.

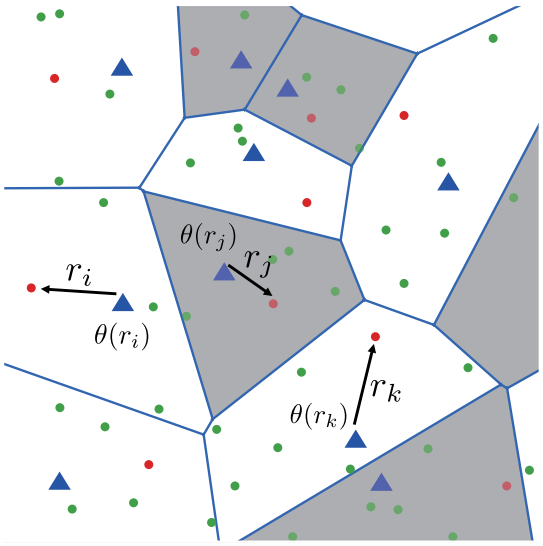

FIGURE 1. System model. Blue triangles represent APs and dots represent STAs. Red dots represent STAs with which the APs try to communicate. APs in the grey area cannot transmit due to carrier sense. Each AP sets the CST based on the communication distance (i.e., average received power).

Each STA is assumed to be associated with the AP with the highest average received signal power, and an AP transmits signals only to one of associated STAs. The locations of the APs are assumed to be distributed according to a PPP $\Phi = \{x_k\}$ with spatial density λ. The communication distance r is assumed to be independent and identically distributed (i.i.d.), and the probability density function (pdf) of the communication distance is given as follows [12]:

$$f_r(r) = 2\pi\lambda r \exp(-\pi\lambda r^2). \tag{1}$$

The coordinate of the STA communicating with the associated AP k is denoted by y_k at a given time.

The channel is assumed to suffer from both path-loss attenuation and Rayleigh fading. The received power at an AP or STA at z from AP k is expressed as follows:

$$p_k A h_{x_k}^{z} \|z - x_k\|^{-\alpha}, \tag{2}$$

where p_k denotes the transmission power of AP k. Parameters A, α, and $\|\cdot\|$ represent the propagation loss at a distance of 1 m, the path loss exponent, and Euclidean distance, respectively. Random variable $h_{x_k}^{z}$ denotes the fading coefficient between AP or STA at z and AP k. The fading coefficient is assumed to be independently, identically, and exponentially distributed with unit mean. Hence, the pdf of the fading coefficient h is given by

$$f_h(h) = \exp(-h). \tag{3}$$

Each AP is assumed to adjust its CST according to its path loss $\|y_k - x_k\|^{-\alpha} = r_k^{-\alpha}$ estimated from the average received power,

$$PA\|y_k - x_k\|^{-\alpha} = PAr_k^{-\alpha}, \tag{4}$$

TABLE 2. Whether AP k with (x_k, r_k, m_k) can transmit when there are other APs $(x, r, m) \in \tilde{\Phi} \setminus (x_k, r_k, m_k)$.

	$m_k \le m$	$m_k > m$
$p(r)Ah_x^{x_k}\|x_k - x\|^{-\alpha} < \theta(r_k)$	Transmit	Transmit
$p(r)Ah_x^{x_k}\|x_k - x\|^{-\alpha} \ge \theta(r_k)$	Transmit	Defer

where r_k represents the communication distance between AP k and associated STA and P represents the initial transmission power of all APs. Note that adjusting the CST according to each average received signal power has been a strategy in previous studies [1], [2] as an approach to throughput improvement.[1] Relation (4) implies that the CST adjustment according to the average received power is equivalent to that according to the communication distance. In this paper, adjusted CST is expressed as a function of communication distance r_k, i.e., $\theta(r_k)$.

The transmission power of AP k is assumed to be determined by the IPS, where the product of the CST and transmission power is constant, as follows:

$$p(r_k) = \frac{P\Theta}{\theta(r_k)}, \quad \forall k, \tag{5}$$

where Θ denotes the initial CST of all APs.

In IEEE 802.11 [13], each AP determines whether it can transmit according to the power received from other APs and backoff counter. Let the random backoff counter of AP k be denoted by m_k. As in [11], m_k is assumed to be a random variable uniformly distributed on [0, 1], i.e., the pdf of the counter m_k is given by

$$f_{m_k}(m_k) = \mathbb{1}(0 \le m_k \le 1), \quad \forall k, \tag{6}$$

where $\mathbb{1}(\cdot)$ is an indicator function that returns one if it is true and zero otherwise. Let $\tilde{\Phi} := \{(x, r, m)\}$ denote a marked PPP consisting of APs that attempt to transmit. As in [11] and summarized in Table 2, AP k is assumed to transmit when backoff counter m_k is smaller than or equal to the counter of other AP, or the received power from other AP is smaller than the CST, $\theta(r_k)$. According to Table 2, whether AP k can transmit is indicated by the medium access indicator e_k expressed as (7), as shown at the bottom of the next page. The medium access indicator is a random variable that is one when the AP is allowed to transmit by the CSMA/CA protocol and zero otherwise.

III. FORMULATION AND NUMERICAL RESULTS OF MAP, CP, AND DST

This section derives the DST. The DST expresses the mean number of successful transmissions per unit area [11], [14].

[1] In detail, previous studies [1], [2] assumed that the CST is adjusted based on the average power received from the furthest associated STA. In contrast, this paper assumes that the CST is adjusted based on the average power received from their communicating STAs at a given time.

The DST is expressed as follows:

$$\begin{aligned} DST &= \lambda\,\mathbb{P}(e_0 = 1 \wedge SINR_0 > T) \\ &= \lambda\,\mathbb{P}(e_0 = 1)\,\mathbb{P}(SINR_0 > T \mid e_0 = 1) \\ &\overset{(a)}{=} \lambda\,\mathbb{E}[e_0]\,\mathbb{P}(SINR_0 > T \mid e_0 = 1), \end{aligned} \tag{8}$$

where $\mathbb{E}[e_0]$, $SINR_0$, T, and $\mathbb{P}(SINR_0 > T \mid e_0 = 1)$ denote the MAP, signal-to-interference-plus-noise power ratio (SINR), SINR threshold for correct signal reception, and the CP of a typical AP, respectively. In this analysis, this paper focuses on a typical AP and considers the probability of instantaneously successful transmission of this typical AP at a given time, and the density of the transmission success APs is given by the product of this probability and density of APs. The MAP represents the probability that an AP is allowed to transmit by the CSMA/CA protocol. Transformation (a) is due to the fact that e_0 takes zero or one. On the contrary, the CP represents the probability that the SINR at the STA communicating with its associated AP is larger than the threshold T. The SINR at STA 0 is given by

$$SINR_0 = \frac{p(r_0) A h_{x_0}^{y_0} r_0^{-\alpha}}{\sigma^2 + I_0}, \tag{9}$$

where I_0, σ^2, and r_0 denote the sum of interference from transmitting APs except AP 0, the noise power, and the communication distance of a typical AP, respectively.

Because the DST is expressed as the product of AP density, MAP, and CP, we first derive the MAP (10) and CP (14), as shown at the bottom of this page in Sections III-A and III-B, respectively. From these derivations, we formulate the DST (17) in Section III-C.

A. MEDIUM ACCESS PROBABILITY (MAP)

Proposition 1: The MAP is given as:

$$\mathbb{E}[e_0] = \int_0^\infty \frac{1 - \exp(-n(r_0))}{n(r_0)} f_r(r_0)\,\mathrm{d}r_0, \tag{10}$$

where

$$n(r_0) = 2\pi\lambda \int_0^\infty \int_0^\infty u \exp\left(-\frac{\theta(r)\,\theta(r_0)}{P\Theta A u^{-\alpha}}\right) f_r(r)\,\mathrm{d}r\,\mathrm{d}u. \tag{11}$$

Proof: The proof is given in Appendix A. □

In particular, when $\alpha = 4$, the integration with respect to u in (11) can be calculated, and $n(r_0)$ is expressed as follows:

$$n(r_0) = \theta(r_0)^{-1/2} N, \tag{12}$$

$$N := \frac{\lambda \pi^{3/2} (P\Theta A)^{1/2}}{2} \int_0^\infty \theta(r)^{-1/2} f_r(r)\,\mathrm{d}r. \tag{13}$$

The integration with respect to r_0 and r in (10) and (13) can be calculated by determining the CST function $\theta(\cdot)$. In particular, the closed-form expression is acquired when the constant or step function is adopted as the CST function.

B. COVERAGE PROBABILITY (CP)

Proposition 2: The CP is given by (14)*, where* $\mathcal{L}_{I_0}(Ta(r_0) r_0^\alpha / PA \mid r_0, e_0 = 1)$ *represents the Laplace transform of* I_0*, given in Lemma 1.*

Proof: The proof is given in Appendix B. □

Lemma 1: The transform of the pdf of the sum of the interference from transmitting APs I_0*,* $\mathcal{L}_{I_0}(Ta(r_0) r_0^\alpha / PA \mid r_0, e_0 = 1)$*, is given in* (15)*, as shown at the bottom of this page.*

Proof: The proof is given in Appendix C. □

As in the MAP, when $\alpha = 4$, the integration with respect to u in (15) can be calculated, and $\mathcal{L}_{I_0}(a(r_0) T r_0^\alpha / PA \mid r_0, e_0 = 1)$ can be calculated as (16), as shown at the bottom of this page.

C. DENSITY OF SUCCESSFUL TRANSMISSIONS (DST)

Proposition 3: The DST is given as:

$$\begin{aligned} DST = \lambda \int_0^\infty \frac{1 - \exp(-n(r_0))}{n(r_0)} \exp\left(\frac{-T\,\theta(r_0)\, r_0^\alpha \sigma^2}{P\Theta A}\right) \\ \times \mathcal{L}_{I_0}\left(\frac{T\,\theta(r_0)\, r_0^\alpha}{P\Theta A} \,\middle|\, r_0, e_0 = 1\right) f_r(r_0)\,\mathrm{d}r_0. \end{aligned} \tag{17}$$

$$\begin{aligned} e_k &= \prod_{(x,r,m) \in \tilde{\Phi} \setminus \{(x_k, r_k, m_k)\}} \mathbb{1}\left(m_k \le m \vee p(r) A h_x^{x_k} \|x_k - x\|^{-\alpha} < \theta(r_k)\right) \\ &= \prod_{(x,r,m) \in \tilde{\Phi} \setminus \{(x_k, r_k, m_k)\}} \mathbb{1}\left(m_k \le m \vee (m_k > m \wedge p(r) A h_x^{x_k} \|x_k - x\|^{-\alpha} < \theta(r_k))\right) \\ &= \prod_{(x,r,m) \in \tilde{\Phi} \setminus \{(x_k, r_k, m_k)\}} \left[\mathbb{1}(m_k \le m) + \mathbb{1}(m_k > m)\,\mathbb{1}\left(p(r) A h_x^{x_k} \|x_k - x\|^{-\alpha} < \theta(r_k)\right)\right], \end{aligned} \tag{7}$$

$$\mathbb{P}(SINR_0 > T \mid e_0 = 1) = \int_0^\infty \frac{1 - \exp(-n(r_0))}{n(r_0)\,\mathbb{E}[e_0]} \exp\left(\frac{-T\,\theta(r_0)\, r_0^\alpha \sigma^2}{P\Theta A}\right) \mathcal{L}_{I_0}\left(\frac{T\,\theta(r_0)\, r_0^\alpha}{P\Theta A} \,\middle|\, r_0, e_0 = 1\right) f_r(r_0)\,\mathrm{d}r_0, \tag{14}$$

$$\mathcal{L}_{I_0}\left(\frac{T\,\theta(r_0)\, r_0^\alpha}{P\Theta A} \,\middle|\, r_0, e_0 = 1\right) \approx \exp\left(-2\pi\lambda \int_{r_0}^\infty \int_0^\infty \frac{1 - \exp(-n(r))}{n(r)} \frac{\theta(r_0)\, T r_0^\alpha u^{-\alpha}}{\theta(r) + \theta(r_0)\, T r_0^\alpha u^{-\alpha}} f_r(r)\, u\,\mathrm{d}r\,\mathrm{d}u\right), \tag{15}$$

$$\mathcal{L}_{I_0}\left(\frac{T\,\theta(r_0)\, r_0^4}{P\Theta A} \,\middle|\, r_0, e_0 = 1\right) \approx \exp\left(-\frac{\pi\lambda\,\theta(r_0)^{1/2}\, T^{1/2} r_0^2}{N\Theta^{1/2}} \int_0^\infty \left(1 - \mathrm{e}^{-N/\theta(r)^{1/2}\,\Theta^{1/2}}\right) \arctan\left(\frac{\theta(r_0)\, T}{\theta(r)}\right)^{1/2} f_r(r)\,\mathrm{d}r\right). \tag{16}$$

TABLE 3. Parameters used in this paper.

P	23 dBm
Θ	-82 dBm
frequency band	5 GHz band
A	-47 dB
σ^2	-100 dBm
α	4

TABLE 4. Parameters in Section III.

a	20 dB
T	10, 20 dB
λ	$0.01, 0.001, 0.0001\ /\mathrm{m}^2$

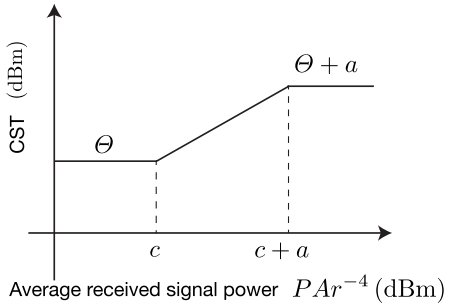

FIGURE 2. CST function $\theta^{(1)}(r)$.

Note that $\mathcal{L}_{I_0}(T\,\theta(r_0)\,r_0^{\alpha}/P\Theta A\,|\,r_0, e_0 = 1)$ *and* $n(r_0)$ *are given in* (15) *and* (11)*, respectively.*

Proof: The DST is the product of the AP density, MAP (10), and CP (14), derived in Sections III-A and III-B, respectively. □

D. NUMERICAL RESULTS

In this section, the numerical evaluation of the derived MAP, CP, and DST is performed. We compare the numerical results with those of a Monte Carlo simulation. This section uses the CST function proposed in [2] as $\theta(\cdot)$. In Section IV, the trend of the optimal CST function for the received power is obtained based on the stochastic geometry. In this paper, parameter values in Table 3 are adopted in all sections. This section also uses the parameter values in Table 4.

In detail, the CST function is set as shown in Fig. 2 seen in dynamic sensitivity control [2] with the CST limited between Θ and $\Theta + a$, where a denotes the maximum increment in the CST. The CST as a function of the communication distance $\theta^{(1)}(r)$ is expressed as follows:

$$\theta^{(1)}(r) = \begin{cases} \Theta + a, & r < \dfrac{(PA)^{1/4}}{10^{(c+a)/40}}; \\ \dfrac{PAr^{-4}}{10^{(c-\Theta)/10}}, & \dfrac{(PA)^{1/4}}{10^{(c+a)/40}} \le r < \dfrac{(PA)^{1/4}}{10^{c/40}}; \\ \Theta, & \dfrac{(PA)^{1/4}}{10^{c/40}} \le r, \end{cases} \tag{18}$$

where c denotes a parameter. Assuming that the CST is set according to dynamic sensitivity control [2], the CST is expressed as follows:

$$\theta^{(2)}(r) = \frac{PAr^{-4}}{M}, \tag{19}$$

where M denotes the margin of dynamic sensitivity control. The CST function $\theta^{(1)}(r)$ (18) is obtained by setting M to $c - \Theta$ and limiting the CST $\theta^{(2)}(r)$ in (19) between Θ and $\Theta + a$. In other words, the margin M is $c - \Theta$. The units of a and c are dB and dBm, respectively.

We present the analytical results together with those of the Monte Carlo simulation with 10,000 trials. Fig. 3 shows the results of the derived DST and the simulation when the density of APs is set to $\lambda = 0.0001, 0.001, 0.01\ /\mathrm{m}^2$. From this figure, it is clear that the DST depends on AP density

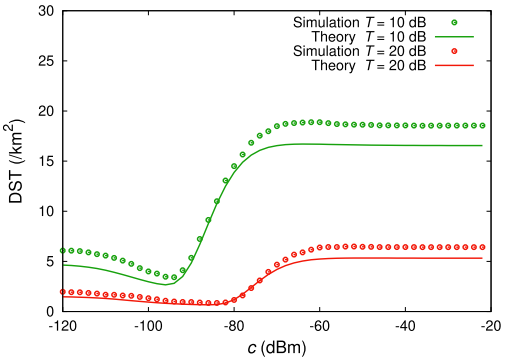

(a) $\lambda = 0.0001\ /\mathrm{m}^2$.

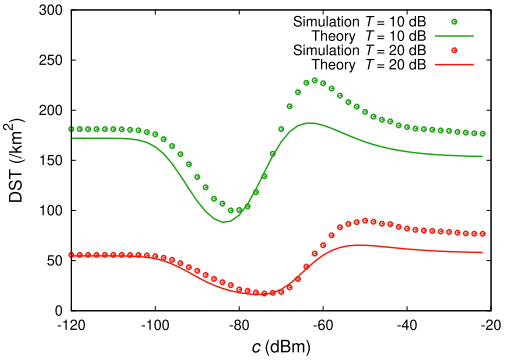

(b) $\lambda = 0.001\ /\mathrm{m}^2$.

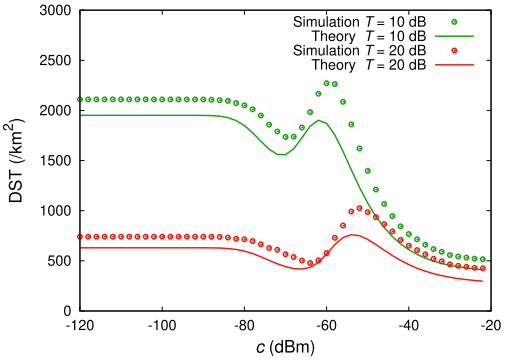

(c) $\lambda = 0.01\ /\mathrm{m}^2$.

FIGURE 3. DST.

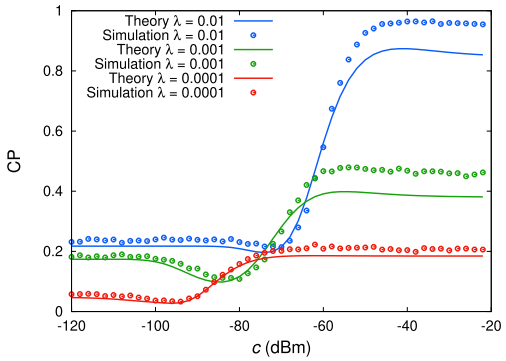

(a) $\lambda = 0.0001\ /\mathrm{m}^2$.

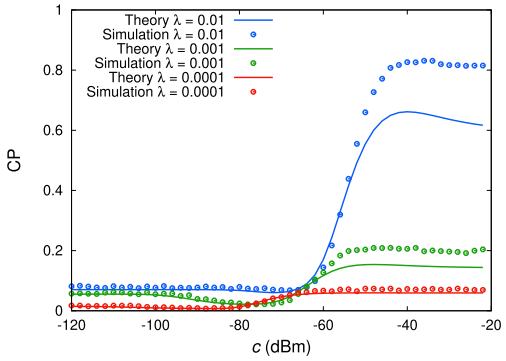

(b) $\lambda = 0.001\ /\mathrm{m}^2$.

FIGURE 4. CP.

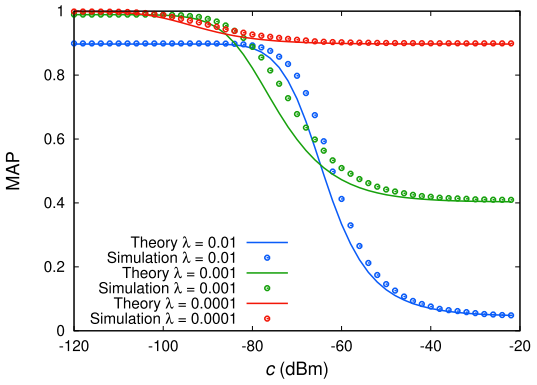

FIGURE 5. MAP.

and c. When the AP density is small, as shown in Fig. 3(a), a large c provides a large value of the DST because the DST relies mainly on the CP, which is increased by the large transmission power as shown in Fig. 4. This is because the MAP is almost always one in any c as shown in Fig. 5. On the contrary, when the AP density is large as shown in Fig. 3(c), a large DST is obtained with a small c because the MAP sharply decreases with an increase in c as shown in Fig. 5.

Almost all results have the largest DST around $c = 60$ dBm because the CP increases rapidly instead of the MAP according to c for any given AP density. Hence, there are some value of c where the CP is large although the MAP is not small. These parameters provide the largest DST. The value of the DST heavily relies on c as AP density increases. Thus, the optimal setting of the CST is more important for high AP density.

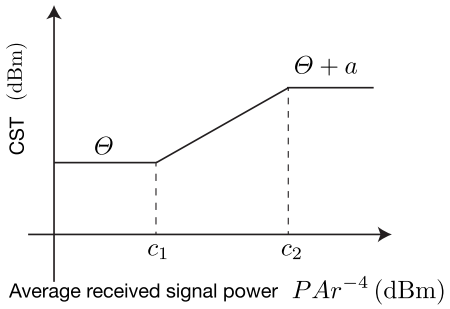

FIGURE 6. Continuous CST function $\theta^{(4)}(r)$.

The CST can be optimized according to the derived DST because the results of simulation and analysis have the same trend, although the former are slightly larger than the latter. Although there is a gap in the absolute value of the DST between the analytical and simulation results, there is no problem from the viewpoint of parameter setting because the parameter taking the maximum or minimum DST is almost identical. This gap is due to the approximation used in the derivation of the DST. In particular, the assumption that each communication distance is i.i.d. assumed in Section II and the approximated locations of interfering APs with a PPP in the derivation (37) are major factors of the gap. The assumption that the communication distance is i.i.d. produces a gap in the MAP as shown in Fig. 5. On the contrary, the gap in the CP in Fig. 4 is due to the approximated locations of interfering APs with a PPP.

IV. OPTIMAL SETTING OF CST IN STEP FUNCTION

This section confirms that the optimal CST increased almost linearly with respect to the average received signal power as shown in Fig. 6 based on stochastic geometry. We attempt to acquire a trend of the optimal CST function using the step function as the CST function, as shown in Fig. 7. The step CST function is given by

$$\theta^{(3)}(r) = b_i, \quad l_i \le r < l_{i+1}, \ i = 1, 2, \ldots, m. \tag{20}$$

Two optimization problems are formulated, and the optimal CST function is acquired by solving the optimization problem. One maximizes the DST, and can be carried out simply. However, this DST maximization produces unfairness. The other one, instead of DST maximization, is intended to maximize the product of the transmission success probabilities over all APs. In Section IV-A, the transmission success probability when the step function is adopted is first derived. In Section IV-B, we formulate two optimization problems. In Section IV-C, we find the optimal function of the CST acquired by solving the optimization problems using the eight-step function.

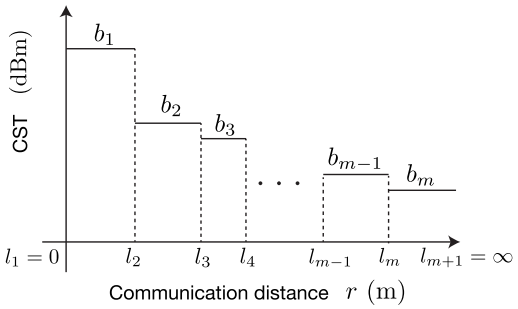

FIGURE 7. CST function $\theta^{(3)}(r)$ adopted in Section IV.

A. TRANSMISSION SUCCESS PROBABILITY IN STEP FUNCTION

To formulate the optimization problem, this section derives the transmission success probability of each AP. By introducing the step function shown in Fig. 7 as the CST function, the transmission success probability of each AP is derived as follows:

$$d_i = \frac{1-\exp\left(-n(l_i)\right)}{s_i\, n(l_i)} \int_{l_i}^{l_{i+1}} \exp\left(-\frac{Tb_i\sigma^2 r_0^{\alpha}}{P\Theta A}\right) \mathcal{L}_{I_0}\left(\frac{Tb_i r_0^{\alpha}}{P\Theta A}\,\middle|\, r_0, e_0 = 1\right) f_r(r_0)\,\mathrm{d}r_0, \quad (21)$$

where s_i denotes the probability that the communication distance is between l_i and l_{i+1}, i.e.,

$$\begin{aligned} s_i &= \mathbb{P}(l_i \le r < l_{i+1}) \\ &= \exp(-\pi\lambda {l_i}^2) - \exp(-\pi\lambda {l_{i+1}}^2). \end{aligned} \quad (22)$$

Proof: The proof is given in Appendix D. □

B. FORMULATION OF OPTIMIZATION PROBLEMS

Using the derived DST (17), optimization problems are formulated to optimize the CST. Using the step function as CST function, this paper finds the trend of the CST maximizing the DST. Parameters maximizing the DST are acquired by solving the following optimization problem:

$$\begin{aligned} &\underset{(\boldsymbol{b},\boldsymbol{l})}{\text{maximize}}\ DST \overset{(\mathrm{l})}{=} \lambda s_1 d_1 + \lambda s_2 d_2 + \cdots + \lambda s_m d_m \\ &\text{subject to } \Theta \le b_i \le \Theta + a, \quad i = 1, \ldots, m \\ &\qquad l_1 = 0 < l_2 < \cdots < l_m < l_{m+1} = \infty. \end{aligned} \quad (23)$$

Transformation (l) is due to the fact that the DST is regarded as the sum of the transmission success probabilities.

The parameter setting maximizing the DST causes unfair channel access in terms of transmission success. This is because DST maximization causes APs with long communication distances to face difficulties while the transmission of APs that have short communication distances becomes easier. In other words, the optimization problem (23) provides $\theta^{(3)}(r)$ with the largest DST while all d_i are large except d_m, so that, the APs that adjust b_m as their CSTs rarely succeed in transmission. In the results, for APs with long communication distances, adjusting the CST according to the DST results in a reduction in their own transmission success probability.

TABLE 5. Parameters in Section IV.

a	21 dB
T	10 dB
λ	$0.005\,/\mathrm{m}^2$

To correct the unfairness of transmission opportunities resulting from maximizing the DST, this paper proposes an alternative optimization problem that maximizes the product of transmission success probabilities. The maximization of the product of the transmission success probabilities instead of the sum of probabilities, i.e., DST, has been discussed in [15]. The product maximization is formulated as follows:

$$\begin{aligned} &\underset{(\boldsymbol{b},\boldsymbol{l})}{\text{maximize}} \prod_{i=1}^{m} d_i^{\lambda s_i} \\ &\text{subject to } \Theta \le b_i \le \Theta + a, \quad i = 1, \ldots, m \\ &\qquad l_1 = 0 < l_2 < \cdots < l_m < l_{m+1} = \infty. \end{aligned} \quad (24)$$

Note that the objective function of (24) is equivalent to $\sum_{i=1}^{m} \lambda s_i \log d_i$, i.e., (24) is doing proportionally fair setting. This optimization problem corrects the unfairness because the objective function becomes very small when one of the transmission success probabilities is very small, so that the solution of this optimization problem provides a large DST while avoiding the situation where some transmission success probabilities are very small.

C. OPTIMIZED CST WITH STEP FUNCTION

This paper attempts to acquire the trend of the optimal CST by solving the optimization problems. This section uses the parameters in Tables 3 and 5, here we set a to be a multiple of 3 dB. Fixing parameter l_i, the optimization problems are numerically solved. Parameter l_i is set assuming that all s_i for $i = 1, 2, \ldots, m$ have the same value. Note that l_i is given by

$$l_i = \sqrt{\frac{\log(m/(m+1-i))}{\pi\lambda}}, \quad i = 1, 2, \ldots, m+1. \quad (25)$$

The results of eight-step function, i.e., $m = 8$, are shown. Fig. 8 shows the optimal CST function according to the average received signal power obtained by solving the optimization problems. In the DST maximization, the CSTs of APs that have long or short communication distances is set large compared with those with medium communication distances. On the contrary, in the product maximization, the optimal CST is reduced with increasing communication distance.

The results of the eight-step function show that the optimal setting is to increase the CST *linearly* with respect to the average received signal power. Fig. 9 shows each transmission success probability for the index of CST function i. In the DST maximization, APs that have long communication distances rarely succeed in transmission, although the transmission success probability of APs that have short communication distances is considerably large. This is because

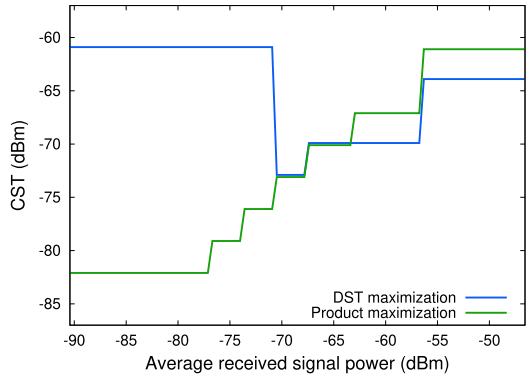

FIGURE 8. Optimal CST $\theta^{(3)}(r)$ according to average received signal power in eight-step function.

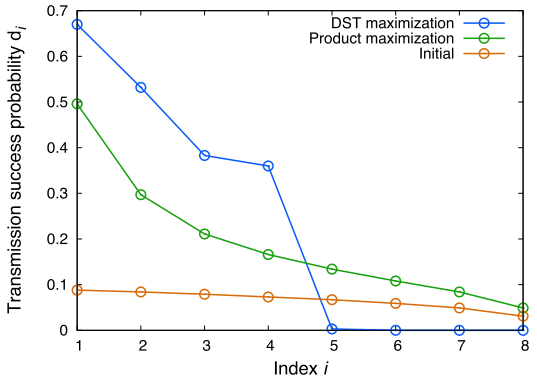

FIGURE 9. Transmission success probability d_i in eight-step function.

APs that have long communication distances set small transmission powers and refrain from interfering with other APs. Hence, the unfairness of transmission opportunities comes about in DST maximization. On the contrary, the product maximization provides a large transmission success probability on the whole compared with the default setting. Therefore, to optimize the CST, product maximization (24) is superior to DST maximization (23).

V. OPTIMAL SETTING OF CST FUNCTION FOR AP DENSITY

This paper optimizes the CST function by using the continuous function shown in Fig. 6. Section IV has indicated that the optimal CST increases almost linearly with respect to the average received signal power. The CST function is given by

$$\theta^{(4)}(r) = \begin{cases} \Theta + a, & r < \dfrac{(PA)^{1/4}}{10^{c_2/40}}; \\ \dfrac{(PAr^{-4})^{\frac{a}{c_2-c_1}}}{10^{\frac{\Theta}{10}-\frac{c_1 a}{10(c_2-c_1)}}}, & \dfrac{(PA)^{1/4}}{10^{c_2/40}} \le r < \dfrac{(PA)^{1/4}}{10^{c_1/40}}; \\ \Theta, & \dfrac{(PA)^{1/4}}{10^{c_1/40}} \le r, \end{cases} \tag{26}$$

where c_1 and c_2 are parameters. The form of the function was introduced in [2]. Parameters c_1 and c_2 maximizing the product of transmission probabilities of all APs are obtained by

TABLE 6. Parameters in Section V.

a	$20\,\mathrm{dB}$
T	$10\,\mathrm{dB}$
λ	$0.01, 0.005, 0.001\,/\mathrm{m}^2$

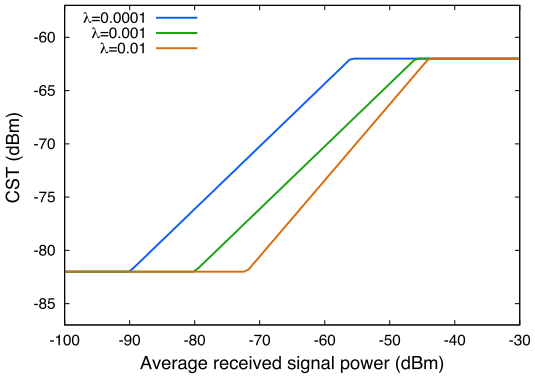

FIGURE 10. Optimal CST function $\theta^{(4)}(r)$ for the AP density.

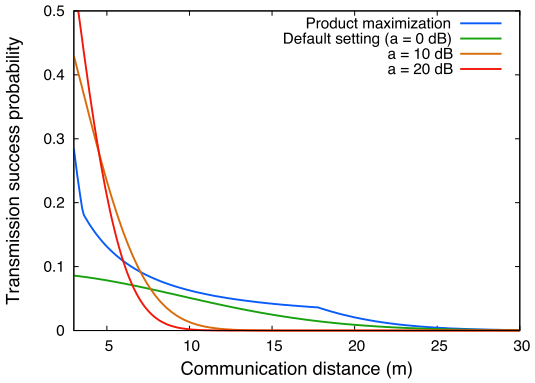

FIGURE 11. Transmission success probability according to communication distance. The green, orange, and red lines show the results when all APs set the CST to −82, −72, −62 dB, respectively.

solving the optimization problem. The problem is expressed as follows:

$$\begin{aligned} &\underset{(c_1,c_2)}{\text{maximize}} \ \lambda \int_0^\infty \log(d(r)) f_r(r)\,\mathrm{d}r \\ &\text{subject to} \ \ c_1 \le c_2, \end{aligned} \tag{27}$$

where $d(r)$ denotes the transmission success probability of the AP with communication distance r.

Proof: The objective function of (27) and the transmission success probability $d(r)$ are given in Appendix E. □

The optimization problem is numerically solved. In solving it, it is assumed that c_1 and c_2 can take an even number between 20 and 120. The other parameters are set as shown in Tables 3 and 6.

Fig. 10 shows the optimal CST obtained by solving the optimization problem (27). The optimal CST function depends on AP density. The optimal parameters c_1 and c_2 increase with an increase in AP density.

Fig. 11 shows the transmission success probability according to the communication distance when $\lambda = 0.005$. Fig. 11 indicates that the proposed setting improves the transmission success probability of almost all APs compared with the default setting, i.e., all CSTs are -82 dBm. Compared with the results when all APs set the same CST, the proposed setting prevents a sharp decrease in the transmission success probability. In other words, from the viewpoint of fairness, the proposed setting is better than the uniform setting.

VI. CONCLUSION

This paper analyzed system performance when APs *individually* adjust the CST according to the average received signal power. The MAP, CP, and DST were derived by using the stochastic geometry framework. The numerical results showed that the DST derived by performing some approximations had the same trend with the simulation results. Thus, we can say that the derived DST is useful to find the optimal CST. To determine the optimal CST, two optimization problems were formulated. By comparing them, it was found that maximizing the product of the transmission success probabilities was more suitable to determine the CST. By using a step function, this paper found that the optimal setting was to increase the CST linearly (in terms of dB) with respect to the average received signal power. Therefore, by using the continuous CST function, the optimal CST for the given AP density was determined.

APPENDIX A

Proof of Proposition 1. We first define $L(x_0, x, r, h_x^{x_0}, m)$ as in [11] as follows:

$$\begin{aligned} &L(x_0, x, r, h_x^{x_0}, m) \\ &:= \mathbb{1}((p(r)Ah_x^{x_0}\|x_0 - x\|^{-\alpha} \geq \theta(r_0)) \wedge (m < m_0)) \\ &= \mathbb{1}(P\Theta Ah_x^{x_0}\|x_0 - x\|^{-\alpha} \geq \theta(r)\,\theta(r_0))\,\mathbb{1}(m < m_0). \end{aligned} \tag{28}$$

Function $L(x_0, x, r, h_x^{x_0}, m)$ represents the probability that AP 0 defers its transmission because it detects a transmission from the AP whose mark is (x, r, m). We also define $X(x_0)$ as follows:

$$X(x_0) = \max_{(x,r,m)\in\tilde{\Phi}} L(x_0, x, r, h_x^{x_0}, m). \tag{29}$$

$L(x_0, x, r, h_x^{x_0}, m)$ takes zero or one; so $X(x_0)$ also takes zero or one. From Slivnyak's theorem, because $e_0 = 1 - X(x_0)$, the MAP conditioned on m_0 and r_0 is expressed as follows:

$$\begin{aligned} &\mathbb{E}[e_0 \,|\, m_0, r_0] \\ &= 1 - \mathbb{E}[X(x_0) \,|\, m_0, r_0] \\ &= 1 - \mathbb{P}(X(x_0) = 1 \,|\, m_0, r_0) \\ &= \mathbb{P}(X(x_0) = 0 \,|\, m_0, r_0) \\ &= \mathbb{P}(X(x_0) \leq 0 \,|\, m_0, r_0) \\ &\overset{(b)}{=} \exp\Bigg(-\int_{\mathbb{R}^2}\int_0^\infty\int_0^\infty\int_0^\infty \mathbb{1}(L(x_0, x, r, h, m) > 0) \\ &\qquad \times F_r(\mathrm{d}r)\,F_h(\mathrm{d}h)\,F_m(\mathrm{d}m)\,\Lambda(\mathrm{d}x)\Bigg) \\ &\overset{(c)}{=} \exp\Bigg(-\int_{\mathbb{R}^2}\int_0^\infty\int_0^\infty\int_0^\infty \mathbb{1}(L(o, x, r, h, m) = 1) \\ &\qquad \times F_r(\mathrm{d}r)\,F_h(\mathrm{d}h)\,F_m(\mathrm{d}m)\,\Lambda(\mathrm{d}x)\Bigg) \\ &= \exp\Bigg(-\int_0^\infty \mathbb{1}(m < m_0)\,F_m(\mathrm{d}m)\int_{\mathbb{R}^2}\int_0^\infty\int_0^\infty \\ &\qquad \mathbb{1}(P\Theta Ah\|x\|^{-\alpha} \geq \theta(r)\,\theta(r_0))\,F_r(\mathrm{d}r)\,F_h(\mathrm{d}h)\,\Lambda(\mathrm{d}x)\Bigg). \end{aligned} \tag{30}$$

In (b), because $\tilde{\Phi}$ is an independently marked PPP with marks r and m, and also h can be regarded as an additional mark in $\tilde{\Phi}$, Proposition 2.13 of [16] is adopted. In (c), x_0 is set as the origin o because x_0 can be taken arbitrarily. Function F_x shows the distribution function of mark x and Λ shows the intensity function.

The marks in $\tilde{\Phi}$ do not depend on the coordinates of the AP x and, hence, the mark distributions also do not depend on x. Moreover, because the locations of the APs follow a PPP, the following equation holds for the intensity function:

$$\Lambda(\mathrm{d}x) = \lambda\,\mathrm{d}x. \tag{31}$$

Thus, the conditional MAP is represented as follows:

$$\begin{aligned} &\mathbb{E}[e_0 \,|\, m_0, r_0] \\ &= \exp\Bigg(-\lambda\int_0^1 \mathbb{1}(m < m_0)\,\mathrm{d}m\int_{\mathbb{R}^2}\int_0^\infty\int_0^\infty \\ &\qquad \mathbb{1}(P\Theta Ah\|x\|^{-\alpha} \geq \theta(r)\,\theta(r_0))f_r(r)f_h(h)\,\mathrm{d}r\,\mathrm{d}h\,\mathrm{d}x\Bigg) \\ &\overset{(d)}{=} \exp\Bigg(-2\pi\lambda m_0\int_0^\infty\int_0^\infty u\exp\left(-\frac{\theta(r)\,\theta(r_0)}{P\Theta Au^{-\alpha}}\right)f_r(r)\,\mathrm{d}r\,\mathrm{d}u\Bigg) \\ &= \exp\left(-m_0\,n(r_0)\right). \end{aligned} \tag{32}$$

Transformation (d) follows [17]. Because m_0 and r_0 are independent, the MAP is derived as follows:

$$\begin{aligned} \mathbb{E}[e_0] &= \int_0^1\int_0^\infty \mathbb{E}[e_0 \,|\, m_0, r_0]f_r(r_0)\,\mathrm{d}r_0\,\mathrm{d}m_0 \\ &= \int_0^\infty f_r(r_0)\int_0^1 \exp(-m_0\,n(r_0))\,\mathrm{d}m_0\,\mathrm{d}r_0. \end{aligned} \tag{33}$$

By integrating with respect to m, the MAP (10) is acquired.

APPENDIX B

Proof of Proposition 2. The CP is rewritten as

$$\begin{aligned} &\mathbb{P}(SINR_0 > T \,|\, e_0 = 1) \\ &= \int_0^\infty \mathbb{P}\left(SINR_0 > T \,|\, r_0, e_0 = 1\right) f_r(r_0 \,|\, e_0 = 1)\,\mathrm{d}r_0 \\ &= \int_0^\infty \mathbb{P}\left(h_{x_0}^{y_0} > \frac{(\sigma^2 + I_0)T\theta(r_0)r_0^\alpha}{P\Theta A}\,\middle|\, r_0, e_0 = 1\right) \\ &\qquad \times f_r(r_0 \,|\, e_0 = 1)\,\mathrm{d}r_0 \\ &\overset{(e)}{=} \int_0^\infty \exp\left(-\frac{T\theta(r_0)\sigma^2 r_0^\alpha}{P\Theta A}\right) \\ &\qquad \times \mathcal{L}_{I_0}\left(\frac{T\theta(r_0)r_0^\alpha}{P\Theta A}\,\middle|\, r_0, e_0 = 1\right)f_r(r_0 \,|\, e_0 = 1)\,\mathrm{d}r_0. \end{aligned} \tag{34}$$

Transformation (e) occurs because the fading coefficient $h_{x_0}^{y_0}$ is assumed to be exponentially distributed with unit mean [17]. The posterior pdf $f_r(r_0 \mid e_0 = 1)$ is expressed from Bayes' theorem as follows:

$$\begin{aligned} f_r(r_0 \mid e_0 = 1) &= \frac{\mathbb{P}(e_0 = 1 \mid r_0) f_r(r_0)}{\mathbb{P}(e_0 = 1)} \\ &= \frac{\mathbb{E}[e_0 \mid r_0] f_r(r_0)}{\mathbb{E}[e_0]} \\ &\overset{(f)}{=} \frac{1 - \exp(-n(r_0))}{n(r_0)\,\mathbb{E}[e_0]} f_r(r_0). \end{aligned} \tag{35}$$

Transformation (f) occurs by integrating (32) with respect to m. This formula indicates that the communication distance for transmitting AP has a distribution different from the original because the CST varies according to communication distance.

APPENDIX C

Proof of Lemma 1. Let $\tilde{\Phi}'$ denote a marked point process, which consists of transmitting APs, i.e., $\tilde{\Phi}' = \{(x_k, r_k, m_k) \in \tilde{\Phi} : e_k = 1\}$. The pdf of the communication distance of the transmitting APs r_k where $(x_k, r_k, m_k) \in \tilde{\Phi}'$ is given similarly to that in (35) as follows:

$$f_{r_k}(r_k \mid e_k = 1) = \frac{1 - \exp(-n(r_k))}{n(r_k)\,\mathbb{E}[e_k]} f_r(r_k). \tag{36}$$

Therefore, all communication distances are mutually independent and have the same pdf $f_r(r \mid e = 1)$. The distributions of the fading coefficients are identical in $\tilde{\Phi}$ and $\tilde{\Phi}'$.

The interference power at STA 0, I_0, is the sum of interference from APs consisting of $\tilde{\Phi}'$ except AP 0. For the derivation, $\tilde{\Phi}'$ is approximated to a PPP $\tilde{\Phi}''$ with density $\lambda' = \lambda\,\mathbb{E}[e_0]$. $\mathbb{E}[e_0]$ indicates the MAP denoted in Section III-A. Such an approximation has also been used in previous studies [8], [11]. From the assumptions, $\mathcal{L}_{I_0}$ is rearranged as follows:

$$\begin{aligned} &\mathcal{L}_{I_0}(s \mid r_0, e_0 = 1) \\ &= \mathbb{E}_{\tilde{\Phi}'}\left[\exp\left(-sI_0\right)\right] \\ &\approx \mathbb{E}_{\tilde{\Phi}''}\left[\exp\left(-sI_0\right)\right] \\ &\overset{(g)}{=} \mathbb{E}_{\Phi''}\left[\prod_{x \in \Phi'' \setminus \{x_0\}} \mathbb{E}_{h,r}\left[\exp\left(-\frac{sP\Theta A h \|y_0 - x\|^{-\alpha}}{\theta(r)}\right)\right]\right] \\ &\overset{(h)}{=} \exp\Bigg(-\lambda\,\mathbb{E}[e_0] \int_{\mathbb{R}^2 \setminus B(y_0, r_0)} \\ &\qquad \left(1 - \mathbb{E}_{h,r}\left[\exp\left(-\frac{sP\Theta A h \|y_0 - x\|^{-\alpha}}{\theta(r)}\right)\right]\right) \mathrm{d}x\Bigg), \end{aligned} \tag{37, 38}$$

where $B(y_0, r_0)$ denotes a two-dimensional ball of radius r_0 centered at y_0 and Φ'' denotes the unmarked PPP in relation to the marked PPP $\tilde{\Phi}''$. Transformation (g) follows from the fact that the fading coefficients are i.i.d. This also applies to r of $(x, r, m) \in \tilde{\Phi}'$. In (h), the probability generating functional for the PPP [18] is used because Φ'' is a PPP. Moreover, the integration domain is $\mathbb{R}^2 \setminus B(y_0, r_0)$ because there are no APs in the range of radius r_0 centered at the coordinates of STA 0 y_0 [17]. The second line of (38) is rearranged as follows:

$$\begin{aligned} &\int_{\mathbb{R}^2 \setminus B(y_0, r_0)} \left(1 - \mathbb{E}_{h,r}\left[\exp\left(-\frac{sP\Theta A h \|y_0 - x\|^{-\alpha}}{\theta(r)}\right)\right]\right) \mathrm{d}x \\ &\overset{(i)}{=} \int_{\mathbb{R}^2 \setminus B(y_0, r_0)} \left(1 - \mathbb{E}_r\left[\frac{1}{1 + sP\Theta A \|y_0 - x\|^{-\alpha}/\theta(r)}\right]\right) \mathrm{d}x \\ &= \int_{\mathbb{R}^2 \setminus B(0, r_0)} \int_0^\infty \frac{sP\Theta \|x\|^{-\alpha}}{\theta(r) + sP\Theta \|x\|^{-\alpha}} f_r(r \mid e = 1)\,\mathrm{d}r\,\mathrm{d}x \\ &= 2\pi \int_{r_0}^\infty \int_0^\infty \frac{sP\Theta A u^{-\alpha}}{\theta(r) + sP\Theta A u^{-\alpha}} f_r(r \mid e = 1)\, u\,\mathrm{d}r\,\mathrm{d}u. \end{aligned} \tag{39}$$

Transformation (i) is due to the assumption that the fading coefficient h follows an exponential distribution.

APPENDIX D

Transmission Success Probability in Step Function. When the step function as shown as Fig. 7 is used as the CST function, the MAP of APs whose communication distances are between l_i and l_{i+1} is given as

$$\begin{aligned} &\mathbb{E}[e_0 \mid l_i \le r_0 < l_{i+1}] \\ &\quad = \frac{\int_0^1 \int_{l_i}^{l_{i+1}} \mathbb{E}[e_0 \mid m_0, r_0] f_r(r_0)\,\mathrm{d}r_0\,\mathrm{d}m_0}{\int_{l_i}^{l_{i+1}} f_r(r_0)\,\mathrm{d}r_0} \\ &\quad = \frac{1}{s_i} \int_{l_i}^{l_{i+1}} f_r(r_0) \int_0^1 \exp(-m_0 n(r_0))\,\mathrm{d}m_0\,\mathrm{d}r_0 \\ &\quad \overset{(j)}{=} \frac{1}{s_i} \int_{l_i}^{l_{i+1}} f_r(r_0)\,\mathrm{d}r_0 \int_0^1 \exp(-m_0\, n(l_i))\,\mathrm{d}m_0 \\ &\quad = \frac{1 - \exp(-n(l_i))}{n(l_i)}. \end{aligned} \tag{40}$$

Transformation (j) is due to the fact that the CST is constant for $l_i \le r_0 < l_{i+1}$. The CP of APs whose communication distances are between l_i and l_{i+1} is rewritten as

$$\begin{aligned} &\mathbb{P}(SINR_0 > T \mid e_0 = 1 \wedge l_i \le r_0 < l_{i+1}) \\ &\quad = \frac{\mathbb{P}(SINR_0 > T \wedge e_0 = 1 \wedge l_i \le r_0 < l_{i+1}) \,/\, \mathbb{P}(e_0 = 1)}{\mathbb{P}(e_0 = 1 \wedge l_i \le r_0 < l_{i+1}) \,/\, \mathbb{P}(e_0 = 1)} \\ &\quad = \frac{\mathbb{P}(SINR_0 > T \wedge l_i \le r_0 < l_{i+1} \mid e_0 = 1)}{\mathbb{P}(l_i \le r_0 < l_{i+1} \mid e_0 = 1)} \\ &\quad = \frac{\int_{l_i}^{l_{i+1}} \mathbb{P}\left(SINR_0 > T \mid r_0, e_0 = 1\right) f_r(r_0 \mid e_0 = 1)\,\mathrm{d}r_0}{\int_{l_i}^{l_{i+1}} f_r(r_0 \mid e_0 = 1)\,\mathrm{d}r_0} \\ &\quad \overset{(k)}{=} \frac{\int_{l_i}^{l_{i+1}} \mathbb{P}\left(SINR_0 > T \mid r_0, e_0 = 1\right) f_r(r_0)\,\mathrm{d}r_0}{\int_{l_i}^{l_{i+1}} f_r(r_0)\,\mathrm{d}r_0} \\ &\quad = \frac{1}{s_i} \int_{l_i}^{l_{i+1}} \exp\left(-\frac{Tb_i \sigma^2 r_0^\alpha}{P\Theta A}\right) \\ &\qquad \mathcal{L}_{I_0}\left(\frac{Tb_i r_0^\alpha}{P\Theta A} \,\middle|\, r_0, e_0 = 1\right) f_r(r_0)\,\mathrm{d}r_0. \end{aligned} \tag{41}$$

Transformation (k) is due to (35) and the fact that $n(r_0)$ is constant for $l_i \leq r_0 < l_{i+1}$. The transmission success probability is formulated by the product of (40) and (41).

APPENDIX E

Derivation of Objective Function of Optimization Problem and Transmission Success Probability in Continuous CST Function. The objective function of (27) is formulated based on the objective function of (24). We first take the logarithm of the objective function of (24).

$$\log \prod_{i=1}^{m} d_i^{\lambda s_i} = \lambda \sum_{i=1}^{m} s_i \log(d_i). \tag{42}$$

When m approaches infinity, s_i is expressed as follows:

$$\begin{aligned}
&\lim_{m\to\infty} s_i \\
&= \lim_{m\to\infty} \left(\exp(-\pi\lambda {l_i}^2) - \exp(-\pi\lambda {l_{i+1}}^2)\right) \\
&= \lim_{m\to\infty} \left(\exp(-\pi\lambda {l_i}^2) - \exp(-\pi\lambda (l_i + \Delta r)^2)\right) \\
&= \lim_{m\to\infty} \exp(-\pi\lambda {l_i}^2) \left(1 - \exp(-\pi\lambda(2 l_i\, \Delta r + \Delta r^2))\right).
\end{aligned} \tag{43}$$

By using the feature that Δr approaches zero as m approaches infinity and the Maclaurin expansion, s_i is rewritten as follows:

$$\begin{aligned}
\lim_{m\to\infty} s_i &= \exp(-\pi\lambda r^2)\,(1 - (1 - 2\pi\lambda r\, \Delta r)) \\
&= 2\pi\lambda r\, \Delta r \exp(-\pi\lambda r^2) \\
&= f_r(r)\, \Delta r.
\end{aligned} \tag{44}$$

Thus, the objective function of (27) is given as follows:

$$\begin{aligned}
\lambda \sum_{i=1}^{m} s_i \log(d_i) &= \lambda \lim_{m\to\infty} \sum_{i=1}^{m} \log(d_i) f_r(r)\, \Delta r \\
&= \lambda \int_0^{\infty} \log(d(r)) f_r(r)\, \mathrm{d}r,
\end{aligned} \tag{45}$$

where $d(r)$ denotes the transmission success probability of the AP whose communication distance is r. The function $d(r)$ is expressed as follows:

$$\begin{aligned}
d(r) &= \mathbb{E}[e \mid r]\, \mathbb{P}(SINR > T \mid r, e = 1) \\
&\overset{(\mathrm{m})}{=} \frac{1 - \exp(-n(r))}{n(r)} \exp\left(-\frac{T\,\theta(r)\,\sigma^2\, r^{\alpha}}{P\Theta A}\right) \\
&\quad \times \mathcal{L}_{I_0}\left(\frac{T\,\theta(r)\, r^{\alpha}}{P\Theta A} \,\middle|\, r, e = 1\right).
\end{aligned} \tag{46}$$

Transformation (m) refers to (33) and (34).

ACKNOWLEDGMENT

This article was presented in part at the 2019 IEEE Consumer Communications and Networking Conference.

REFERENCES

[1] M. S. Afaqui, E. Garcia-Villegas, E. Lopez-Aguilera, G. Smith, and D. Camps, "Evaluation of dynamic sensitivity control algorithm for IEEE 802.11ax," in *Proc. IEEE Wireless Commun. Netw. Conf. (WCNC)*, New Orleans, LA, USA, Mar. 2015, pp. 1060–1065.

[2] M. S. Afaqui, E. Garcia-Villegas, E. Lopez-Aguilera, and D. Camps-Mur, "Dynamic sensitivity control of access points for IEEE 802.11ax," in *Proc. IEEE Int. Conf. Commun. (ICC)*, Kuala Lumpur, Malaysia, May 2016, pp. 1–7.

[3] X. Yang and N. Vaidya, "On physical carrier sensing in wireless ad hoc networks," in *Proc. IEEE Int. Conf. Comput. Commun. (INFOCOM)*, Miami, FL, USA, vol. 4, Mar. 2005, pp. 2525–2535.

[4] V. P. Mhatre, K. Papagiannaki, and F. Baccelli, "Interference mitigation through power control in high density 802.11 WLANs," in *Proc. IEEE Int. Conf. Comput. Commun. (INFOCOM)*, Anchorage, AK, USA, May 2007, pp. 535–543.

[5] J. A. Fuemmeler, N. H. Vaidya, and V. V. Veeravalli, "Selecting transmit powers and carrier sense thresholds in CSMA protocols for wireless ad hoc networks," in *Proc. ACM Int. Wireless Internet Conf. (WICON)*, Boston, MA, USA, Aug. 2006, Art. no. 15.

[6] D. Okuhara, F. Shiotani, K. Yamamoto, T. Nishio, M. Morikura, R. Kudo, and K. Ishihara, "Attenuators enable inversely proportional transmission power and carrier sense threshold setting in WLANs," in *Proc. IEEE Int. Symp. Pers., Indoor, Mobile Radio Commun. (PIMRC)*, Washington, DC, USA, Sep. 2014, pp. 986–990.

[7] D. Okuhara, K. Yamamoto, T. Nishio, M. Morikura, and H. Abeysekera, "Inversely proportional transmission power and carrier sense threshold setting for WLANs: Experimental evaluation of partial settings," in *Proc. IEEE Veh. Tech. Conf. (VTC-Fall)*, Montreal, QC, Canada, Sep. 2016, pp. 1–5.

[8] H. ElSawy and E. Hossain, "A modified hard core point process for analysis of random CSMA wireless networks in general fading environments," *IEEE Trans. Commun.*, vol. 61, no. 4, pp. 1520–1534, Apr. 2013.

[9] B. Cho, K. Koufos, and R. Jäntti, "Interference control in cognitive wireless networks by tuning the carrier sensing threshold," in *Proc. IEEE Cognit. Radio Oriented Wireless Netw. (CROWNCOM)*, Washington, DC, USA, Jul. 2013, pp. 282–287.

[10] K. Yamamoto, X. Yang, T. Nishio, M. Morikura, and H. Abeysekera, "Analysis of inversely proportional carrier sense threshold and transmission power setting," in *Proc. IEEE Consum. Commun. Netw. Conf. (CCNC)*, Las Vegas, NV, USA, Jan. 2017, pp. 13–18.

[11] F. Baccelli and B. Błaszczyszyn, "Stochastic geometry and wireless networks: Volume II applications," *Found. Trends Netw.*, vol. 4, nos. 1–2, pp. 1–312, 2009.

[12] H. ElSawy and E. Hossain, "On stochastic geometry modeling of cellular uplink transmission with truncated channel inversion power control," *IEEE Trans. Wireless Commun.*, vol. 13, no. 8, pp. 4454–4469, Aug. 2014.

[13] *IEEE Standard for Information Technology—Telecommunications and Information Exchange Between Systems Local and Metropolitan Area Networks—Specific Requirements—Part 11: Wireless LAN Medium Access Control (MAC) and Physical Layer (PHY) Specifications*, IEEE Standard 802.11-2016, Dec. 2016.

[14] Y. Li, F. Baccelli, J. G. Andrews, T. D. Novlan, and J. C. Zhang, "Modeling and analyzing the coexistence of Wi-Fi and LTE in unlicensed spectrum," *IEEE Trans. Wireless Commun.*, vol. 15, no. 9, pp. 6310–6326, Sep. 2016.

[15] F. Baccelli, B. Błaszczyszyn, and C. Singh, "Analysis of a proportionally fair and locally adaptive spatial aloha in Poisson networks," in *Proc. IEEE Int. Conf. Comput. Commun. (INFOCOM)*, Toronto, ON, Canada, Apr. 2014, pp. 2544–2552.

[16] F. Baccelli and B. Błaszczyszyn, "Stochastic geometry and wireless networks, volume I—theory," *Found. Trends Netw.*, vol. 3, nos. 3–4, pp. 249–449, 2009.

[17] J. G. Andrews, F. Baccelli, and R. K. Ganti, "A tractable approach to coverage and rate in cellular networks," *IEEE Trans. Commun.*, vol. 59, no. 11, pp. 3122–3134, Nov. 2011.

[18] M. Haenggi, *Stochastic Geometry for Wireless Networks*. Cambridge, U.K.: Cambridge Univ. Press, 2012.

MOTOKI IWATA received the B.E. degree in electrical and electronic engineering from Kyoto University, in 2017, and the M.I. degree from the Graduate School of Informatics, Kyoto University, in 2019.

KOJI YAMAMOTO (S'03–M'06) received the B.E. degree in electrical and electronic engineering from Kyoto University, in 2002, and the M.E. and Ph.D. degrees in informatics from Kyoto University, in 2004 and 2005, respectively. From 2004 to 2005, he was a Research Fellow of the Japan Society for the Promotion of Science (JSPS). Since 2005, he has been with the Graduate School of Informatics, Kyoto University, where he is currently an Associate Professor. From 2008 to 2009, he was a Visiting Researcher with the Wireless@KTH, Royal Institute of Technology (KTH), Sweden. His research interests include radio resource management and applications of game theory. He received the PIMRC 2004 Best Student Paper Award, in 2004, the Ericsson Young Scientist Award, in 2006. He also received the Young Researcher's Award, the Paper Award, SUEMATSU-Yasuharu Award from the IEICE of Japan, in 2008, 2011, and 2016, respectively, and IEEE Kansai Section GOLD Award, in 2012. He serves as an Editor of the IEEE Wireless Communications Letters, in 2017, and the Track Co-Chairs of APCC 2017 and CCNC 2018.

BO YIN received the B.E. degree in electrical and electronic engineering from Kyoto University, in 2016, and the M.E. degree from the Graduate School of Informatics, Kyoto University, in 2018, where he is currently pursuing the Ph.D. degree. He received the VTS Japan Young Researcher's Encouragement Award, in 2017.

TAKAYUKI NISHIO (M'87) received the B.E. degree in electrical and electronic engineering from Kyoto University, Kyoto, Japan, in 2010, and the master's and Ph.D. degrees in communications and computer engineering from the Graduate School of Informatics, Kyoto University, in 2012 and 2013, respectively. From 2012 to 2013, he was a Research Fellow (DC1) of the Japan Society for the Promotion of Science (JSPS). Since 2013, he has been an Assistant Professor in communications and computer engineering with the Graduate School of Informatics, Kyoto University. From 2016 to 2017, he was a Visiting Researcher with the Wireless Information Network Laboratory (WINLAB), Rutgers University, USA. His current research interests include mmWave networks, wireless local area networks, application of machine learning, and sensor fusion in wireless communications. He is a member of the ACM and IEICE. He received IEEE Kansai Section Student Award, in 2011, the Young Researcher's Award from the IEICE of Japan, in 2016, and Funai Information Technology Award for Young Researchers, in 2016.

MASAHIRO MORIKURA received the B.E., M.E., and Ph.D. degrees in electronics engineering from Kyoto University, Kyoto, Japan, in 1979, 1981, and 1991, respectively. He joined NTT in 1981, where he was involved in the research and development of TDMA equipment for satellite communications. From 1988 to 1989, he was with the Communications Research Centre, Canada, as a Guest Scientist. From 1997 to 2002, he was active in the standardization of the IEEE 802.11a based wireless LAN. He is currently a Professor with the Graduate School of Informatics, Kyoto University. His current research interests include WLANs and M2M wireless systems. Dr. Morikura received the Paper Award and the Achievement Award from IEICE, in 2000 and 2006, respectively. He also received the Education, Culture, Sports, Science and Technology Minister Award, in 2007 and Maejima Award, in 2008, and the Medal of Honor with Purple Ribbon from Japan's Cabinet Office, in 2015.

HIRANTHA ABEYSEKERA received the B.Eng., M.Eng., and Ph.D. degrees in communications engineering from Osaka University, Japan, in 2005, 2007, and 2010, respectively. He joined NTT Network Innovation Laboratories, Yokosuka, Japan, in 2010, where he was involved in the Research and Development of next-generation wireless LAN systems. He is currently working as a Senior Research Engineer with NTT Access Service Systems Laboratories. His research interests include resource allocation in wireless LANs. He received the IEEE VTS Japan Student Paper Award, in 2009.